Numerical investigation of three-dimensional shock/boundary-layer interaction in a hypersonic inlet

Krishnendu Sinha, Nilesh J. Rane, and Vighnesh Pawar

1 Introduction

In a hypersonic inlet, the incoming flow is compressed through a series of oblique shocks. The shock waves interact with the boundary layer that forms on the inlet wall, which can cause flow separation. Separation bubbles act as blockage in the inlet duct and can result in problems in starting and high localized heat transfer rate. In three-dimensional configuration, the shock/boundary-layer interaction (SBLI) and resulting flow separation can be quite complex. It is important to understand the flow physics in detail, so as to explore ways of minimizing flow separation and its adverse effect.

An extensive amount of research has been done on three-dimensional SBLI. The most fundamental interaction is observed in a single-fin configuration. The planar shock generated by the fin interacts with the boundary layer on an adjacent plate. The flow field generated by single fin configuration is studied in detail by Panaras [1], Settles [2] and others. The crossing shock wave generated by two fins results in a more complex flow separation pattern on the plate. This double-fin configuration is studied experimentally by Zheltovodov *et al.* [3] and computationally by Gaitonde *et al.* [4].

Three-dimensional SBLI occurring in inlet ducts can often be characterized in terms of canonical flows. In this paper, the flowfield in a practical intake geometry is studied using computational fluid dynamics. The focus is the impingement and reflection of the cowl shock inside the inlet duct, and the resulting SBLI. A previous study [5] presents a detailed analysis of the three-dimensional shock structure and flow separation in a simplified duct geometry. The current work extends the analysis to a real-life configuration.

Department of Aerospace Engineering, Indian Institute of Technology Bombay
Mumbai-400076, India

2 Configuration

The intake geometry considered in this work is shown in Fig. 1. It consists of an external compression part with two forebody ramps of 10.5^o deflection each. It is followed by three expansion corners that lead to the inlet duct. The cowl is deflected by 4^o with a hinge located 150 mm downstream of the cowl lip. A side fence is used to avoid spillage over the edges of the forebody ramps. The width of the duct is 120 mm in the spanwise direction. The freestream conditions correspond to $M = 6.5$, $p = 2$ kPa and $T = 220$ K. A schematic of the shocks formed on the forebody ramps and inlet duct is shown in the figure.

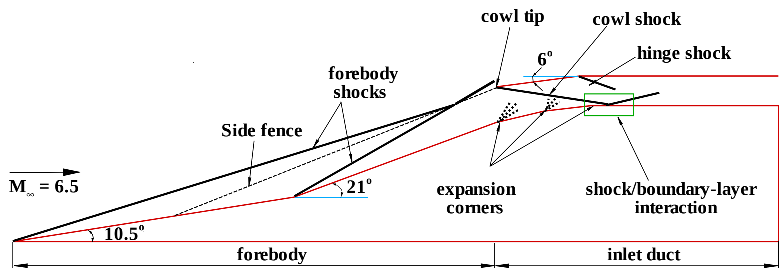

Fig. 1 Intake configuration showing geometric details and representative shocks and expansion waves.

3 Simulation Methodology

We solve three-dimensional Reynolds-averaged Navier-Stokes (RANS) equations and the Spalart-Allmaras (SA) model [6] is used in the simulations for turbulence closure. In-house code [7] based on finite-volume formulation of the governing equations and a modified low-dissipation form of the Steger-Warming flux-splitting approach is used. The discretization method is second-order accurate in space. An implicit method is used to integrate in time and reach a steady-state solution. The code has been validated for several supersonic and hypersonic flow applications.

The computational domain (Fig. 2) consists of the intake duct, starting slightly upstream of the cowl tip. The forebody ramps are simulated separately and the flow-field solution downstream of the ramp shocks is prescribed as inlet condition to the current duct simulation. The boundary-layer on the ramp is also included in the inlet profile. Due to symmetry of the problem, only half of the geometry is simulated in the spanwise direction and symmetry conditions are applied at the center-plane.

A structured Cartesian grid, shown in Fig. 2, is used to span the inlet duct. A total of 8×10^6 points are used with 200 points each in the streamwise and transverse

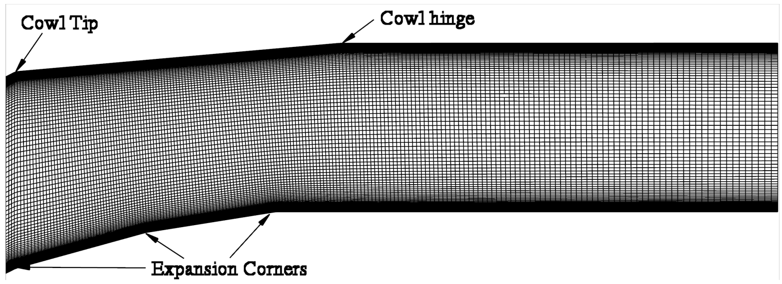

Fig. 2 Simulation domain and computational grid shown at the symmetry plane.

directions. The half-width of the duct is spanned by 150 points. The grid points are clustered in critical regions like the cowl tip, expansion corners, shocks and SBLI zones. The wall-normal spacing adjacent to the intake walls is set at 1μm, which results in a $y_2^+ \leq 1.7$ throughout the geometry. The grid resolution is comparable to that used in Ref. [5], for which a detailed grid refinement study has been performed.

4 Simulation results

The flow pattern in the symmetry plane is shown in Fig. 3. The impingement of the cowl shock on the opposite wall results in a typical oblique SBLI, described in Ref. [8]. It leads to a complex pattern of shocks and expansion waves inside the duct. Additional features include the expansion fans formed at the entry of the duct, and a weak shock generated at the cowl hinge.

The cowl shock also interacts with the boundary layer on the side wall to form a quasi-conical separation zone, which is similar to that seen in a single-fin interaction. The separation and reattachment lines are marked as S_1 and R_1 in Fig. 4. Note that cowl shock is bent due to the expansion fans formed at the duct entry. As a result, the whole conical separation region on the side wall is curved downwards.

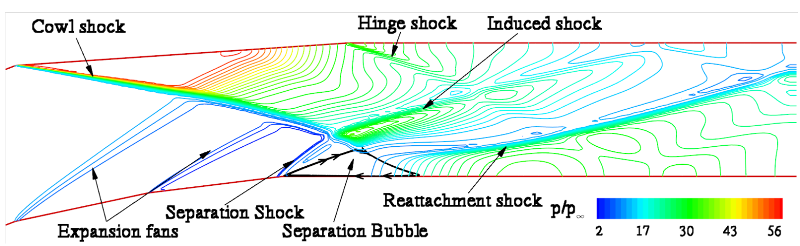

Fig. 3 Computed pressure contour plotted in a streamwise plane along the duct center line

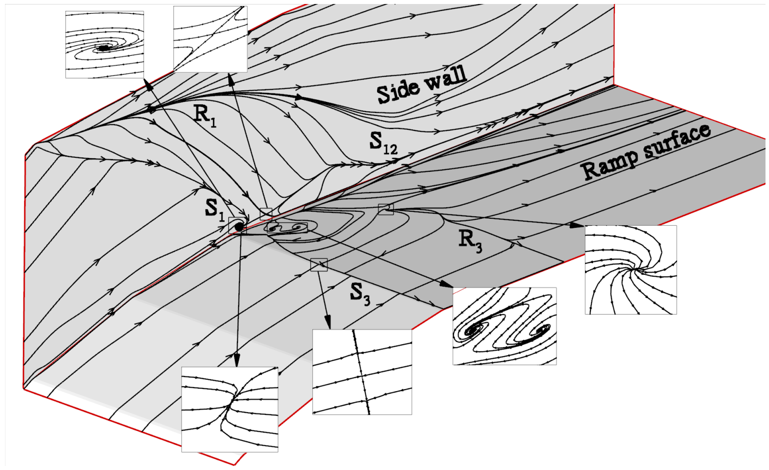

Fig. 4 Limiting surface streamlines plotted on the side wall & ramp surface

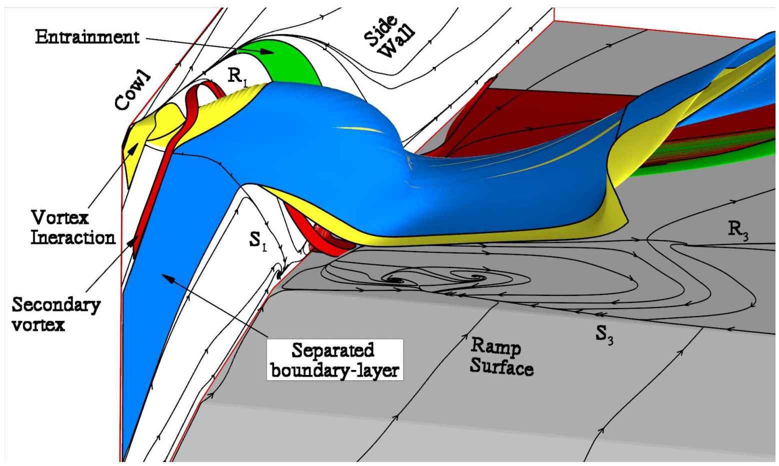

Fig. 5 Different flow regimes [4] are identified in terms of computed stream surfaces.

The lines S_3 and R_3 in Fig. 4 represent flow separation and reattachment on the ramp surface, where the region between the two lines corresponds to the separation bubble. The limiting surface streamlines at the junction of the ramp and side walls show a complex pattern. It is a result of an interaction between the conical vortex on the side wall and the separation bubble on the ramp surface. The flow in the corner region is highly three-dimensional, with multiple flow separation and reattachment lines. For example, line S_{12} on the side wall marks the location of secondary separation, and it represents a longitudinal vortex formed at the corner.

The separation bubble formed on the ramp wall acts as a blockage in the flow, and generates the separation shock wave. The separation shock, along with the cowl shock, forms a crossing-shock/boundary-layer interaction similar to that observed in double-fin configurations. Gaitonde *et al.* [4] study the side-wall interaction in an asymmetric double-fin geometry. They characterize the separated flow region in terms of different flow regimes like, vortex interaction, separated boundary layer and secondary vortex. The same flow regimes can be identified in the current geometry and they are marked in Fig. 5. The critical points in the surface flow pattern Fig. 4 also match those identified in the double-fin configuration and are described in detail by Gaitonde *et al.* [4].

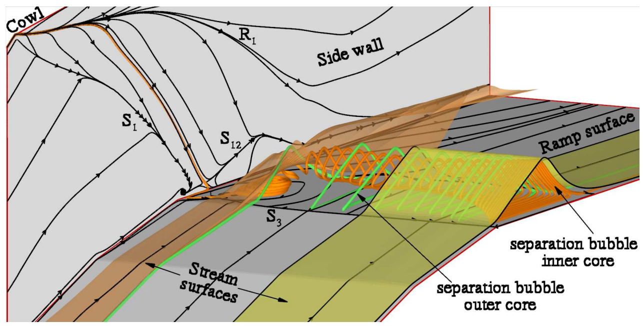

Fig. 6 Volume and surface streamlines showing the structure of the separation bubble.

Figure 6 shows the vortical flow inside the separation bubble that forms on the ramp wall. The fluid in the vortex core, shown by orange streamline, originates in the conical side-wall vortex. It follows along the walls and get ejected from the ramp wall to form a helical structure. The cross-section of the helical vortex at the symmetry plane matches the separation bubble observed in Fig. 3. A similar flow pattern is reported in asymmetric double-fin interaction by Gaitonde et al. The fluid in the outer part of the vortex, shown by green stream line, originates in the ramp boundary layer and it envelops the helical vortex core.

Figure 7 shows the three-dimensional shock structure in several cross planes inside the duct. The top wall (not shown) corresponds to the cowl and the bottom wall is the ramp surface. The left boundary is the side wall, and is omitted from the figure to visualize the shock pattern in the vicinity of the corner. The duct flow is dominated by the cowl shock, which is initially planar. Near the side wall, the cowl shock bifurcates into a lambda structure that envelops the conical vortex. This is typical of a single-fin interaction. The shape of the separation shock formed on the ramp wall is visible in the later cross-section, and it interacts with the lambda structure. The last section also shows the planar shock generated by the cowl hinge, and the expansion waves formed at the beginning of the duct are visible in the first section.

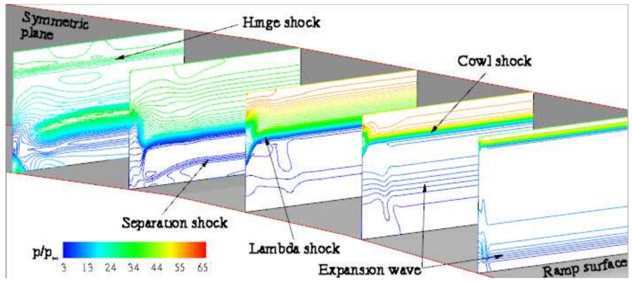

Fig. 7 Computed pressure contours plotted on cross sectional planes.

5 Conclusion

The current paper presents a numerical study of the three-dimensional flowfield inside a practical hypersonic inlet duct. Impingement of the cowl shock causes flow separation on the opposite wall. The shock wave generated by the separation bubble, along with the cowl shock, results in a crossing-shock/boundary-layer interaction on the side wall. The flowfield exhibits several key features observed earlier in double-fin configurations. Analysis of the the surface streamlines, three-dimensional stream-surfaces and the shock structure gives a detailed understanding of the complex flow pattern inside the inlet duct.

References

1. Panaras A. G., “Review of The Physics of Swept-Shock/Boundary-Layer Interactions”, *Progress in Aerospace Sciences*, Vol. 32, 173-244, 1996.
2. Settles G. S., “Shock-Wave/Boundary Layer Interactions in Supersonic and Hypersonic Flows”, AGARD Report, No. 792, Chap. 1, May 1993.
3. Zheltovodov, A. A., Maksimov, A. I. and Shevchenko, A. M., “Topology of three-dimensional separation under the conditions of symmetric interaction of crossing shocks and expansions waves with turbulent boundary layer”, *Therm. Aero. Mech* , Vol. 5, No. 3, 293-312, 1998.
4. Gaitonde, D. V., Shang J. and Visbal, M., “Side-wall interactions in an Asymmetric Simulated Inlet Configuration”, *Journal of Propulsion and Power*, Vol. 17, No. 3, 579-584, 2001.
5. Pawar, V., Rane, N. and Sinha, K., “Three-dimensional Shock/Turbulent Boundary Layer Interaction in a Simulated Scramjet Inlet,” Symposium on Applied Aerodynamics and Design of Aerospace Vehicle (SAROD 2009) December 10-12, Bangalore, India, 336-343 2009.
6. Spalart, P. R. and Allmaras, S. R., “A One-equation Turbulence Model for Aerodynamic Flows,” *AIAA Paper*, AIAA-92-0439, Reno, NV, Jan. 1992.
7. Sinha, K., Candler, G. V., “Convergence Improvement of Two-Equation Turbulence Model Calculations”, *AIAA Paper*, 98-2649, June 1998.
8. Pasha, A. A. and Sinha, K., “Shock-Unsteadiness Model Applied to Oblique Shock-Wave/Turbulent Boundary-Layer Interaction,” *International Journal of Computational Fluid Dynamics*, Vol. 22, No. 8, 2008, pp. 569-582.